

Influence of impurities on dynamic hysteresis of magnetization reversal

Guang-Ping Zheng and Mo Li

School of Materials Science and Engineering, Georgia Institute of Technology, 771 Ferst Drive, N.W., Atlanta, Georgia 30332

(Received 11 February 2002; revised manuscript received 12 April 2002; published 2 August 2002)

The effects of impurities on driving-rate-dependent energy loss in ferromagnets are investigated by analyzing several well-defined models for magnetization reversal. The random-field Ising models are analyzed using a mean-field approximation and Monte Carlo simulation. The hysteresis loop area A is found to obey a universal scaling relation with respect to the linear driving rates h of the applied field, $A - A_0 \propto h^\beta$. The scaling exponent β is found independent of the disorder strength D . In a random-field spherical model, the energy loss increases as a power law with the driving rate $A \propto h^{\beta(D)}$. The scaling exponent $\beta(D)$ increases with increasing D . These results indicate that the scaling and universality for the field-driven first-order phase transition can be understood in the framework of dynamic hysteresis.

DOI: 10.1103/PhysRevB.66.054406

PACS number(s): 75.40.Gb, 75.60.Ej, 64.60.Cn

I. INTRODUCTION

The field-driven first-order phase transition (FOPT) is one of the most commonly seen phase transitions that have wide technology applications. For example, magnetic hard disks¹ and ferroelectric memory devices² are based on the principles of the first-order phase transition driven by magnetic fields in magnets and electric fields in ferroelectric materials, respectively. In recent years, the dynamic process or the switching dynamics of the field-driven first-order phase transition in information storage devices has been the subject of extensive investigations.^{3,4} The sweeping frequency in these devices often varies over ten decades. For such a vast span in the dynamic response, the corresponding dynamic properties and their physical origins could be considerably different.

The rate-dependent hysteresis loop in the field-driven FOPT has been intensively investigated.⁸ In some model systems, the area of the hysteresis loop in a conjugate coordinates, i.e., the energy loss per swept cycle of the applied field, shows a power-law scaling relation with the driving rate or frequency ω of the applied field: $A = A_0 + a\omega^\beta$, where A_0 is the static hysteresis loop area and β is a system-related scaling exponent. We can put those model systems into three categories based on the scaling exponent β : (1) In dynamic mean-field models governed by Glauber dynamics,⁹ cell dynamics¹⁰ or Ginzburg-Landau dynamics,¹¹ the scaling exponent β is observed to be equal to 2/3. (2) In model systems that are governed by Langevin dynamics, the exponent is determined by the spatial dimensionality and the dimensions of order parameter. For example, in an N -vector model,¹² $\beta = 1/2$ for $N \geq 2$ and $d > 2$; $\beta = 1/3$ for a large- N vector model with $O(N)$ symmetry.¹³ (3) In Ising models, $\beta = 0.36$ (Ref. 14), 0.45 (Ref. 15), and 0.66 (Ref. 16) in two-, three-, and four-dimensional systems, respectively.

The power-law scaling relation between energy dissipation and driving rate has been well confirmed in the model systems mentioned above, under both sinusoidal and linear driving fields. Although there are several exceptions of the non-power-law scaling relation reported, the power-law scaling relation appears to be universal for the field-driven FOPT when the driving rate is low. The power-law scaling relation lasts at least four to five decades. The physical origin of the

scaling for energy dissipation is generally considered to come from the consequence of the coexistence of two phases during FOPT's: the dynamic response of the interfaces between two phases to the external driving field. Nucleation and growth are the fundamental mechanisms for interface motions. The growth of the interface is proposed to be the origin of the power-law scaling for energy dissipation at low sweeping rates, while the nucleation process results in a logarithmic scaling relation between energy loss and the sweeping rates.

In the past several years, experimental studies of this issue have been made possible with the advancement in the preparation of ultrathin films, high-quality single crystals, and low-dimensional array samples. In ferromagnetic thin films, β was observed to vary from 0.0 to 0.66, although the power-law scaling relation is confirmed in at least five decades of driving rates.¹⁷⁻¹⁹ The discrepancy of β between experiments and theoretical predictions was observed and attributed to the magnetic anisotropy of the thin-film materials, the domain nucleation, and domain-wall motions. In ferroelectric samples, this discrepancy is even more significant because of the presence of vacancies and a depleted charge layer.²⁰

Impurities and defects are known to play important roles in the first-order phase transition.⁵⁻⁷ In switching dynamics, rate-dependent hysteresis and energy dissipation are perhaps the two most important nonequilibrium phenomena and are significantly influenced by the presence of defects. However, the effects of impurities on the rate-dependent energy dissipation in the field-driven first-order phase transition have not been well understood to date.

Unlike second-order phase transitions that have well-defined critical scaling and critical exponents, there is no general theory for scaling relations in FOPT's. Based on the above-mentioned model systems and experiment results in the field-driven FOPT, it appears that in order to describe the scaling and universality, we need to consider the dynamic hysteresis or rate-dependent energy dissipation: Both the hysteresis and energy dissipation are two of the most commonly occurring phenomena in FOPT's. By considering these general phenomena, we could explore the possibility of scaling and universality for the energy dissipation in FOPTs. A simple class of the models could be the field-driven FOPT.

Next, we shall consider the influence of impurities on the dynamics of metastable states, which is closely related to the dynamical hysteresis. For the nucleation-controlled or growth-controlled kinetics of FOPTs, the interaction between defects and interfaces and the interaction among interfaces are the two most important mechanisms that cause the discrepancy between theoretical predictions in model systems and experimental measurements in real systems. Up to now there has been no model system that could describe the effect of impurities on the rate-dependent energy dissipation in FOPTs. As we mentioned above, most of the efforts have been focused on defect-free model systems.⁹⁻¹⁶ It is known that in real systems the rate-dependent energy loss in a FOPT caused by the interface kinetics is directly related to defects. They could dramatically affect the motion of interface, depending on the strength of interaction, the defect concentration, and their nature.

In this paper we study several model systems in which the effect of defects is our primary consideration. We shall treat the effect of defects as random fields and analyze the scaling relation between energy dissipation and riving rates in field-driven FOPTs with the presence of these defects. The present work is inspired by the following unanswered questions of dynamic hysteresis. First, what is the universality of hysteresis scaling for FOPT's in some well-defined model systems? Does the power-law scaling relation valid for the system with quenched-in defects? Second, why is the scaling exponent β in real systems different from that of model systems? How does the presence of impurities in field-driven FOPTs affect the exponent β ? To answer these questions, in Sec. III we investigate two exactly solvable model systems: namely a mean-field random-field Ising model (RFIM) and a random-field spherical model. In Sec. III, we calculate exactly the energy dissipation in a three-dimensional random-field Ising model using Monte Carlo simulation. We will give the summary and conclusions in Sec. IV.

II. DYNAMIC SCALING FOR HYSTERESIS IN RANDOM-FIELD MODELS

A. Mean-field approximation for random-field Ising model

By treating the impurities as random fields, we can write the Hamiltonian of the Ising system as

$$\hat{H} = -J \sum_{\langle ij \rangle} S_i S_j - \sum_i h_i S_i - H(t) \sum_i S_i, \quad (1)$$

where $S_i = \pm 1$ are spin variables and $\langle ij \rangle$ denotes the summation extending over all nearest-neighbor spins. H is a homogeneous external magnetic field; h_i is a random field with bimodal distribution $P(h_j) = [\delta(h_j - h_0) + \delta(h_j + h_0)]/2$, where h_0 is the strength of the random field. H , T , and h_0 are in units of exchange interaction strength J .

If the system satisfies the detailed balance condition at finite temperature T and is described by Glauber dynamics, based on the mean-field approximation, the thermal average magnetization $\langle S_j \rangle$ is independent of site j , and the equation of motion can be written as

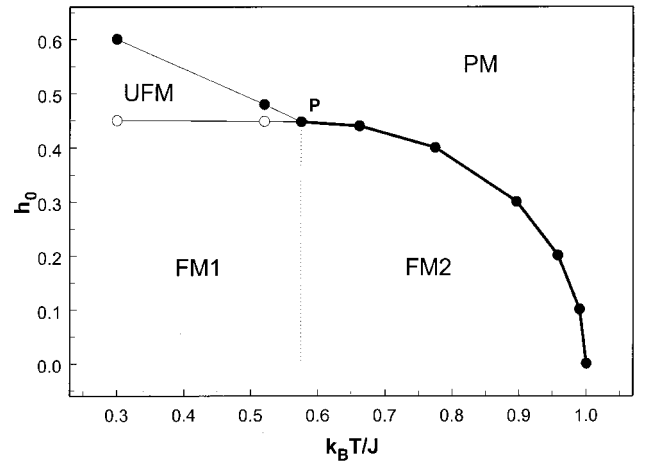


FIG. 1. Phase diagram of a random-field Ising model. FM denotes ferromagnetic phase. PM denotes paramagnetic phase. UFM is the unstable ferromagnetic phase. The thick solid line is the transition line of the second-order phase transition. The thin solid line is the transition line of a first-order phase transition.

$$\frac{d}{dt} \langle S_j \rangle = -\langle S_j \rangle + \langle f(S_j) \rangle, \quad (2)$$

where

$$f(S_j) = \tanh \left[\left(J \sum_i S_i + h_i + H \right) / k_B T \right] \quad (3)$$

is a function of the nearest neighbors of the j th spin. Because the observed magnetization can be written as $m = [\langle S_j \rangle]$, where $[\dots]$ denotes the average over the random-field configurations, Eq. (2) therefore becomes

$$\frac{d}{dt} m = -m + \frac{1}{2} \left[\tanh \left(\frac{Jm + h_0 + H}{k_B T} \right) + \tanh \left(\frac{Jm - h_0 + H}{k_B T} \right) \right]. \quad (4)$$

The phase diagram of the RFIM without applied field is depicted in Fig. 1 by setting the right-hand side of Eq. (4) to zero. (T, h_0) denotes an initial equilibrium phase before the external field is applied. $P(T^t, h_0^t)$ denotes the tricritical point that separates a second-order phase transition from a FOPT. Besides the ferromagnetic and paramagnetic phases, there is a metastable ferromagnetic phase. T_c is the critical temperature at a given h_0 .

The hysteresis loop is obtained by applying a sweeping field to the system. For a pure Ising model with sinusoidal field $H(t) = H_0 \cos \omega t$, the loop area is written as⁹

$$A - A_0(T) \propto H_0^{2/3} \omega^{2/3} g_L(\omega/H_0^\gamma), \quad (5)$$

where $g_L(x)$ is a scaling function, $T < T_c$, and $\gamma = 0.3$. The dynamical hysteresis $A - A_0(T)$ first increases and then decreases with increasing ω for a fixed field amplitude H_0 . In the random-field Ising model, we choose a linear varying field: $H(t) = H_0 - ht$ and $H(t) = -H_0 + ht$, where H_0 is large enough for magnetization saturation and h is defined as a linear driving rate. The advantage of using the linear driv-

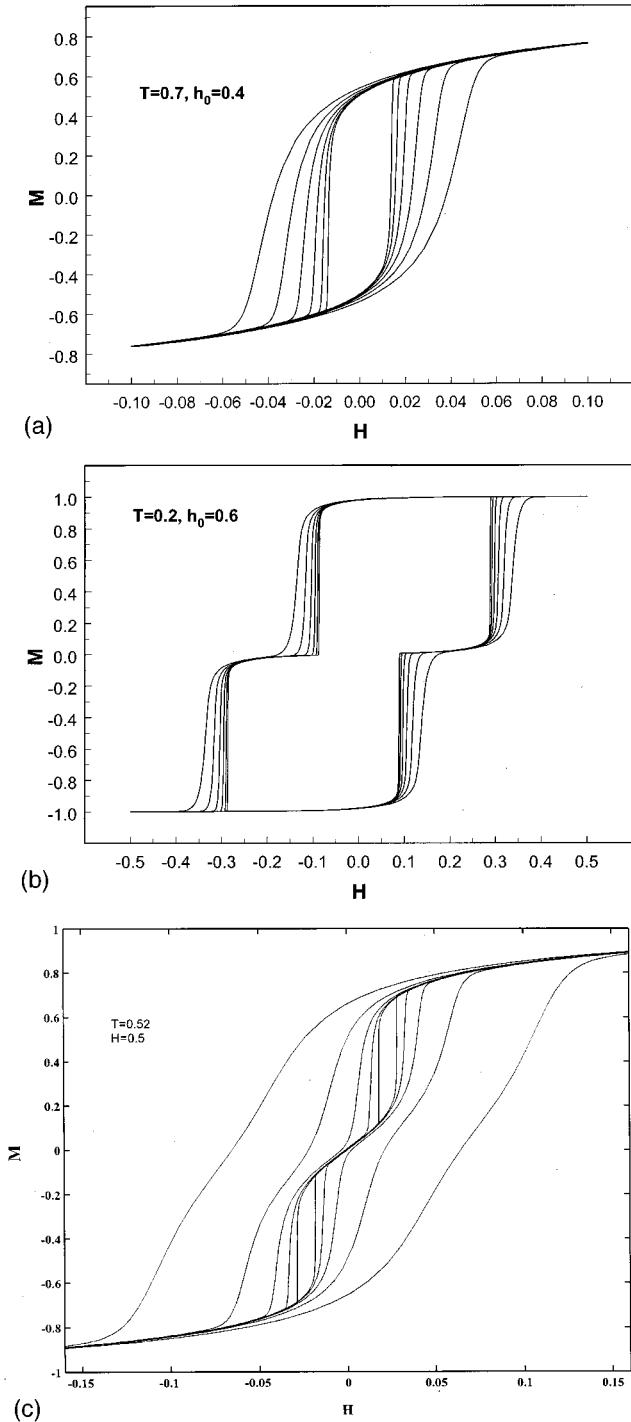


FIG. 2. Hysteresis loops at different linear driving rates in a RFIM. (a) The initial state is in the FM1 or FM2 phase. $h = 0.01, 0.005, 0.0025, 0.00125, 0.000625,$ and 0.0003125 from inner to outer loops. (b) The initial state is in the UFM phase. The driving rates are the same as those in (a). (c) The initial state is in the PM phase. The driving rates are $h = 0.01, 0.0025, 0.000625, 0.00015625,$ and 0.0000244 from inner to outer loops.

ing field is that the hysteresis loop area is independent of H_0 and the scaling for $A(h; T, h_0)$ can be well determined.

Equation (4) is solved using fifth Runge-Kutta formulas. Figure 2 shows the typical hysteresis loops of system with

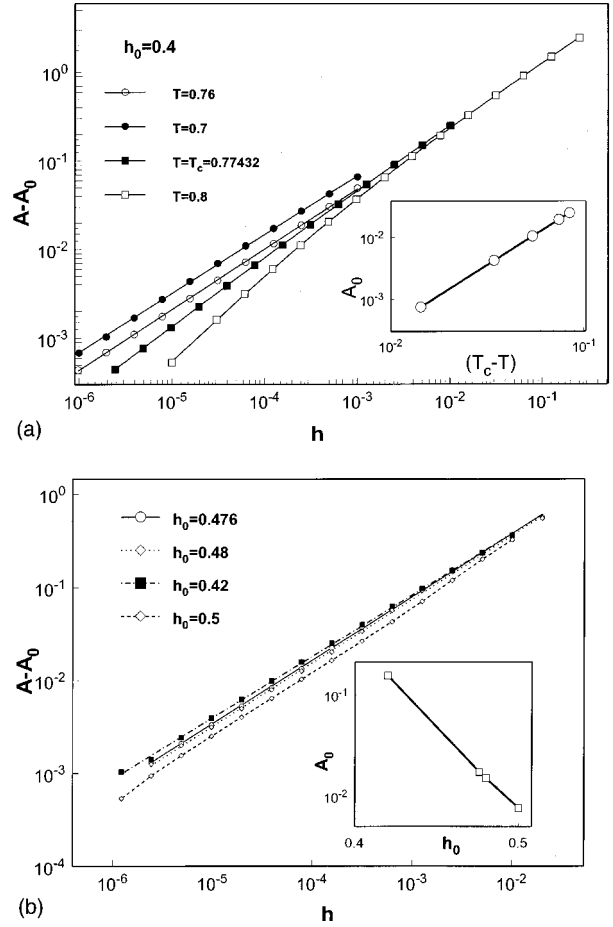


FIG. 3. log-log plots of dynamical hysteresis $A - A_0$ with respect to the driving rates h . (a) At different temperatures and fixed h_0 . The inset is the log-log plot of the static loop area A_0 with $T_c - T$. (b) At different h_0 and fixed T . The inset shows the relation between $\log A_0$ and h_0 .

different initial phases. Comparing those with the pure Ising model, we find that the hysteresis loops in a random-field Ising model have different shapes that are caused by the impurities. Started from an initial ferromagnetic phase (FM phase), the system undergoes a FOPT and generates hysteresis [Figs. 2(a) and 2(b)].

Figure 3(a) shows the effect of temperature on the loop area at small disorder strength. The static loop area $A_0(T, h_0)$ is calculated from Eq. (4) by setting $h = 0$ and $dm/dt = 0$. For the FOPT, i.e., $T < T_c$, the energy loss is a power-law function of the driving rate h :

$$A - A_0(T) \propto h^\beta, \quad A_0 \propto (T_c - T)^\alpha, \quad (6)$$

where $\alpha = 2$ and $\beta = 2/3$ are independent of the disorder. These exponents are the same as those of a pure Ising models. When the initial state is a paramagnetic (PM) phase and h_0 is small—i.e., the hysteresis loop is not caused by FOPTs—the hysteresis loop area can be written as

$$A \propto h^{2/3} / (1 + ah^{\beta'}), \quad (7)$$

where a is a constant and $\beta' < 0$ depends on temperature T and disorder strength h_0 .

For the systems whose initial states are in other regions in the phase diagram, the hysteresis loop area can be written as Eq. (6). Figure 3(b) shows the effect of h_0 on the hysteresis scaling. The inset indicates that the static loop area A_0 is an exponential function of h_0 . If the hysteresis is caused by FOPT's, the exponent β is $2/3$. Although the impurities introduce an unstable state ($M=0$) during the magnetization reversal process as shown in Fig. 2(b), the exponent β is independent of the disorder strength.

B. Random-field spherical model

Consider a three-dimensional model with a random field: the Hamiltonian for a spherical model can be written as

$$\hat{H} = -\frac{J_0}{2} \sum_{i \neq j} S_i S_j - \sum_i H_i S_i, \quad (8)$$

with constraint $\sum_i S_i^2 = N$, where N is the total number of spins and $-\infty < S_i < +\infty$ is a continuous spin variable. $H_i = H + h_i$, and h_i is a Gaussian random field with zero mean and variance h_0^2 . The Langevin dynamics for this constrained system is

$$\frac{\partial \sigma_q}{\partial t} = -\Gamma[\lambda(t) - \beta J_0] \sigma_q + \eta_q(t), \quad (9)$$

where σ_q is the Fourier transform of the spin fluctuation:

$$\sigma_q = \frac{1}{\sqrt{N}} \sum_i (S_i - m) e^{jqr_i}, \quad (10)$$

and $m \equiv [\langle \sum_i S_i \rangle] / N$ is the average magnetization. η_q is a Gaussian white noise:

$$\langle \eta_q \rangle = 0, \quad \langle \eta_q(t) \eta_{-q}(t') \rangle = 2\Gamma \delta(t - t'). \quad (11)$$

In Eq. (9), $\lambda(t)$ is a Lagrange multiplier corresponding to the constraint and Γ is set to 1.

Using the Fokker-Planck equation for constrained system derived by Schwartz,²¹ the Langevin equation (9) leads to the equations of motion for the following physical quantities:

$$\begin{aligned} \frac{dm(t)}{dt} &= -[(1 - J_0/k_B T) + (J_0/k_B T)m^2 + s(t)]m(t) + H, \\ \frac{dC_q(t)}{dt} &= 2\{1 - [(1 - J_0/k_B T) + (J_0/k_B T)m^2 + s(t)] \\ &\quad + q^2\}C_q(t) - h_0^2 \chi_q(t), \\ \frac{d\chi_q(t)}{dt} &= 1 - [(1 - J_0/k_B T) + (J_0/k_B T)m^2 + s(t)] \\ &\quad + q^2\} \chi_q(t), \end{aligned} \quad (12)$$

where

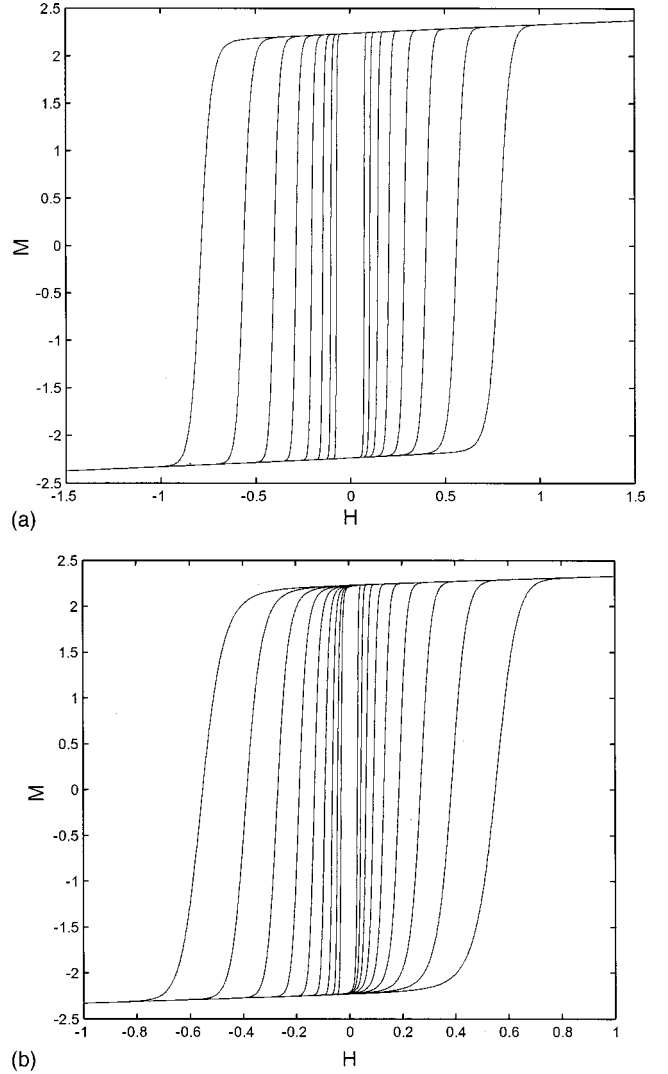


FIG. 4. Hysteresis loops caused by the first-order phase transition in spherical models. $J_0/k_B T = 2$. The driving rates are $h = 0.01, 0.005, 0.0025, 0.00125, 0.000625, 0.0003125, 0.00015625, \text{ and } 0.00007813$. (a) $h_0 = 0.0$ and (b) $h_0 = 4.0$.

$$\begin{aligned} s(t) &= \frac{J_0}{Nk_B T} \left[\sum_q C_q(t) + h_0^2 \chi_q \right], \\ C_q(t) &\equiv [\langle \sigma_{-q}(t) \sigma_q(t) \rangle], \\ \chi_q(t) &\equiv \frac{1}{h_0^2} [h_q \langle \sigma_{-q} \rangle]. \end{aligned} \quad (13)$$

To solve the coupled differential-integral equations (12) and (13) numerically, we use 50-node Gauss-Legendre quadrature and fifth Runge-Kutta formulas for numerical integral and differential, respectively. The system without an applied field is at the ferromagnetic phase when $J_0/k_B T = 2$.

Figure 4 compares the rate-dependent hysteresis loops in the random-field spherical systems with and without impurities. At the same driving rate, the loop area in system with impurities is smaller than that of a pure system. Figure 5

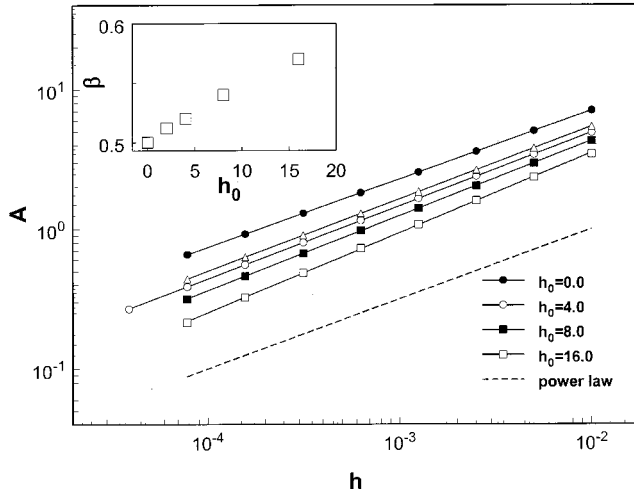


FIG. 5. Relation between hysteresis loop area A and the driving rate h . The plots are in log-log scales. The inset shows the relation between the scaling exponent β and the strength of disorder D .

shows the log-log plots of energy loss (area of hysteresis loop) and the driving rates at different disorder strengths. The energy loss is fitted well to a power-law function of the driving rate:

$$A(T, h_0) \propto h^{\beta(h_0)}. \quad (14)$$

Although the scaling relation [Eq. (14)] is independent of the disorder strength, the scaling exponent β increases with increasing disorder strength h_0 . For strong disorder strength, β is apparently different with $\beta = 1/2$ in an impurity-free system, as shown in the inset of Fig. 5.

The scaling exponent β for the FOPT in this model shares the same features as the critical exponents in a second-order phase transition that are found to be dependent on the disorder strength.²² This important feature suggests that it is possible to describe the scaling and universality for FOPT's using the concept of dynamic hysteresis scaling.

III. DYNAMIC HYSTERESIS IN A THREE-DIMENSIONAL RFIM AT ZERO TEMPERATURE

In the last section, the results from the solvable models indicate that when stochastic kinetics is taken into account, the scaling exponent for the FOPT depends on the disorder strength. In the systems without fluctuations such as the mean-field model, the impurities do not affect the scaling exponent. To explore this finding furthermore, we shall consider other systems that have no thermal fluctuation, but show field-driven FOPT's. The three-dimensional (3D)

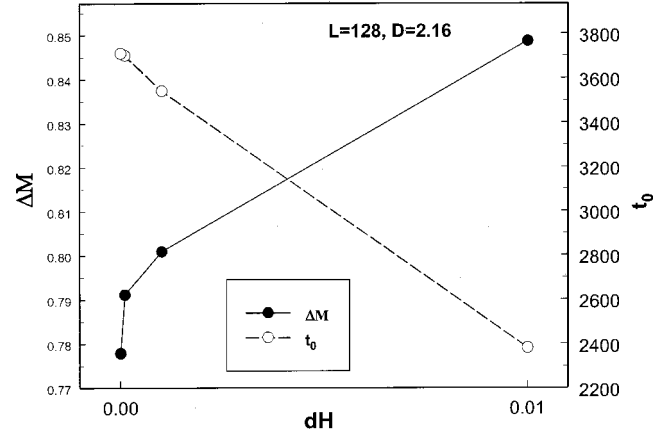


FIG. 6. Dependence of magnetization change ΔM and the duration time t_0 on the field change dH in FOPT's under mode-(b) driving field. The system size of the 3D RFIM is $L=128$ and $D=2.16$.

RFIM at zero temperature is such a system that has been well investigated. We are interested in looking at the effect of disorder on the hysteresis scaling for FOPT's in this system.

The 3D RFIM can be described by Eq. (1). We assume the random field is a Gaussian variable with zero mean and variance D^2 . When $H=0$ the system was shown to have a disorder-driven phase transition at $D_c = 2.16$ at $T=0$.²² When the sweeping field is applied, the hysteresis loops show distinct shapes below and above D_c . If $D > D_c$, the hysteresis loop consists of many small abrupt changes and the overall loop is smooth. If $D < D_c$, there is an obviously discontinuous jump in the hysteresis loop, exhibiting a field-driven FOPT. Because the system is kept at $T=0$, the thermal effect on energy dissipation in the FOPT can be excluded and we are able to focus on the effect of impurities on the hysteresis scaling.

The 3D RFIM described by Eq. (1) is investigated in this work by Monte Carlo simulations. Physical quantities are averaged over 1000–5000 random-field configurations. The system size is $L=128$. To speed up the simulation, a fast algorithm similar to the sort-list algorithm is used. All spins are updated simultaneously. One time step, or one Monte Carlo step (MCS), in the simulation is defined as one attempt of all spin updates. A spin will flip if its local field $f_i = \sum J S_j + h_j + H$ changes sign. The external field is decreased by dH and then is fixed until all spins have been updated. There are three types of driving modes in our simulation studies: (a) An infinite slow driving field or static driving field. In this driving mode dH is adjusted to the minimum

TABLE I. Energy loss and critical field in the 3D RFIM under mode-(a) and mode-(b) driving fields.

Mode	W			H_c		
	$D=1.80$	$D=2.16$	$D=2.33$	$D=1.80$	$D=2.16$	$D=2.33$
(a)	3.132	2.839	2.657	1.586	1.443	1.403
(b)	3.140	2.807	2.650	1.586	1.444	1.403

($dH=10^{-3}$)

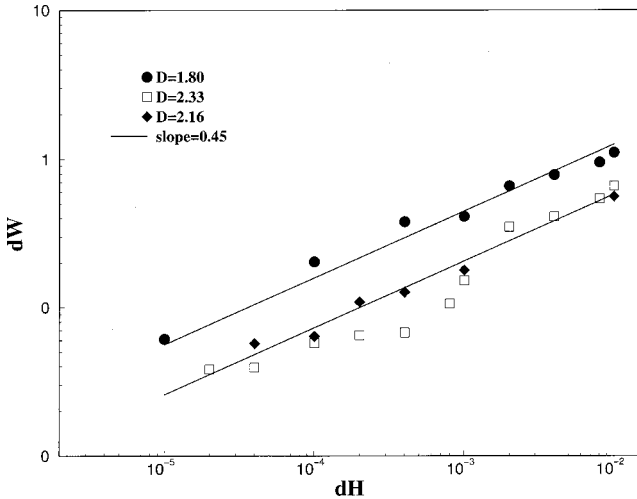


FIG. 7. Relation between dynamical energy loss $dW = W - W_a$ and the linear driving rates in a 3D RFIM. The plots are in log-log scales. The solid lines are power-law curves with exponent 0.45.

local field f_i after a metastable state is reached. (b) Step-function driving field or quasistatic driving field. dH in this driving mode is kept as a constant throughout the magnetization reversal process. It is added to the driving field only after the metastable state is reached. (c) Linear driving field. It is achieved by changing the field by a fixed dH every time step.

The energy loss per sweeping cycle can be derived based on the criterion of a spin flip at $T=0$. The local energy dissipation due to a spin flip can be calculated by

$$dW_i = f_i \Delta S_i, \quad (15)$$

where $\Delta S_i = 0, \pm 2$ is the local spin flip. It is easy to prove that the total energy loss per cycle is equal to the loop area.

$$W = \sum_i^N dW_i = \oint M dH = \sum_{k=1}^n \sum_{j=1}^{N(k)} 2|f_j|, \quad (16)$$

where n is the total number of jumps, $N(k)$ is the number of flip spins in the k th jump, and j labels the flipped spin in the k th jumps.

Under a quasistatic driving mode (step-function driving field), the discontinuous magnetization change ΔM (the largest jump in the loop) and the duration time t_0 of the FOPT are shown in Fig. 6. Table I compares the energy dissipation under the driving modes (a) and (b). H_c is the critical field at which the FOPT occurs, and ΔM is the largest. From Table I we find that the energy loss and the critical field in the system under static driving field—i.e., driving modes (a)—are the same as those in the system driven by a step-function driving field [driving mode (b)]. However, the energy loss in systems driven by a linear driving field [mode (c)] is quite different. Figure 7 shows its dynamic energy dissipation, i.e., $dW = W - W_a$, where W_a is the energy loss under a static driving mode. When there is a FOPT at $D < D_c(L)$, dW can be fitted to a power-law function as in Eq. (6) and the exponent $\beta = 0.44 \pm 0.04$ and $\beta = 0.43 \pm 0.04$ for $D = 1.80$ and $D = 2.16$, respectively. For the system with $D = 2.33$ in which the hysteresis is not generated by a FOPT, the relation be-

tween dW and dH cannot be fitted to Eq. (6). It is interesting to see that the scaling exponent in the 3D RFIM is the same as that of a pure 3D Ising model where $\beta = 0.45$.

IV. SUMMARY AND CONCLUDING REMARKS

Two solvable model systems are employed in this work to investigate the universality of dynamical scaling for field-driven FOPT's with the presence of defects. The mean-field approximation for a random-field Ising model suggests that for a field-driven FOPT at a low driving rate, the dynamical energy loss $A - A_0$ is a power-law function of the linear driving rate. The scaling exponent β is equal to $2/3$ and is independent of the disorder. The dynamical hysteresis that is not caused by the FOPT cannot be expressed by a unique scaling function with respect to the driving rate. When the linear driving rate is high, all dynamical hysteresis can be fitted to a power-law function of the driving rate and the exponent is $2/3$. These results are different from the hysteresis scaling in a mean-field Ising model under a sinusoidal applied field.

In a random-field spherical model, the energy dissipation in FOPT's is also fitted well to a power-law function of the linear driving rate. However, the scaling exponent depends on the disorder strength. The reason why β increases with increasing disorder strength is that the stronger the disorder, the easier for the driving field to drive the system to saturation magnetization, because the impurities introduce additional disorder to the ferromagnetic ordered phase. In the mean-field model, the random field we considered is of short-range correlation: therefore, β is independent of disorder strength.

The scaling for energy dissipation in FOPT's is also investigated by applying Monte Carlo simulations to a deterministic system, a 3D RFIM at zero temperature. Since the hysteresis loop is deterministic for a given random-field configuration, the energy loss can be calculated exactly. Like the mean-field RFIM, in field-driven FOPT's the scaling for the energy loss with respect to the linear driving rate is observed to be independent of disorder strength. The scaling exponent β is also the same as that in a pure 3D Ising model.

In conclusion, we find that in the systems with random-field impurities the scaling for energy dissipation of field-driven FOPT's can be written as $A = A_0 + ah^\beta$. The exponent is independent of the disorder strength when stochastic kinetics is neglected. For the mean-field RFIM, $\beta = 2/3$, and for the 3D RFIM at zero temperature, $\beta = 0.45$. These results are the same as those of corresponding pure systems. For a random-field spherical model, the power-law scaling relation between energy dissipation and linear driving rate holds, but $A_0 = 0$ and the scaling exponent β depends on the disorder strength. These results indicate that it is possible to understand the scaling and universality for FOPT's in the framework of rate-dependent energy dissipation.

ACKNOWLEDGMENTS

Financial support for this work was provided by the Department of Energy under Contract No. DE-FG02-99ER45784 and the Whiting School of Engineering at Johns Hopkins University.

- ¹J. C. Mallinson, *The Foundation of Magnetic Recording* (Academic, San Diego, 1993).
- ²J. F. Scott and C. A. Pazde Araujo, *Science* **246**, 1400 (1989).
- ³K. B. Klaassen and R. G. Hirko, *IEEE Trans. Magn.* **32**, 90 (1996).
- ⁴M. Alexe, A. Gruverman, C. Harnagea, N. D. Zakharov, A. Pignolet, D. Hesse, and J. F. Scott, *Appl. Phys. Lett.* **75**, 1158 (1999).
- ⁵M. A. Bates and D. Frenkel, *Phys. Rev. E* **61**, 5223 (2000).
- ⁶J. Cardy and J. L. Jacobsen, *Phys. Rev. Lett.* **79**, 4063 (1997).
- ⁷E. Kierlik, P. A. Monson, M. L. Rosinberg, L. Sarkisov, and G. Tarjus, *Phys. Rev. Lett.* **87**, 055701 (2001).
- ⁸For a review, see B. K. Chakrabarti and M. Acharyya, *Rev. Mod. Phys.* **71**, 847 (1999).
- ⁹C. N. Luse and A. Zangwill, *Phys. Rev. E* **50**, 224 (1994).
- ¹⁰S. Senguptas, Y. Marathe, and S. Puri, *Phys. Rev. B* **45**, 7828 (1992).
- ¹¹P. Jung, G. Gray, R. Roy, and P. Mandel, *Phys. Rev. Lett.* **65**, 1873 (1990); I. D. Mayergoyz and C. Serpico, *IEEE Trans. Magn.* **36**, 3192 (2000).
- ¹²P. B. Thomas and D. Dhar, *J. Phys. A* **26**, 3973 (1993).
- ¹³M. Rao, *Phys. Rev. B* **42**, 856 (1990).
- ¹⁴W. S. Luo and R. A. Pelcovits, *Phys. Rev. A* **42**, 7471 (1990).
- ¹⁵M. Acharyya and B. K. Chakrabarti, *Phys. Rev. B* **52**, 6550 (1995).
- ¹⁶G. P. Zheng and J. X. Zhang, *J. Phys.: Condens. Matter* **10**, 275 (1998).
- ¹⁷J. S. Suen and J. L. Erskine, *Phys. Rev. Lett.* **78**, 3567 (1997).
- ¹⁸W. Wernsdorfer, E. B. Orozco, K. Hasselbach, A. Benoit, B. Barbara, N. Demoncey, A. Loiseau, H. Pascard, and D. Mailly, *Phys. Rev. Lett.* **78**, 1791 (1997).
- ¹⁹B. C. Choi, W. Y. Lee, A. Samad, and J. A. C. Bland, *Phys. Rev. B* **60**, 11 906 (1999).
- ²⁰D. H. Kin and J. J. Kim, *Ferroelectrics* **222**, 543 (1999).
- ²¹M. Schwartz, *Phys. Lett.* **76A**, 408 (1980); M. Schwartz and Y. Navot, *Physica A* **255**, 318 (1998).
- ²²M. Gofman, J. Adler, A. Aharony, A. B. Harris, and M. Schwartz, *Phys. Rev. B* **53**, 6362 (1996).